Quantifying the Spatial Heterogeneity Relations Between Thermal Environment Effects and Influencing Factors Based on Geodetector in Central City of Chengdu

Yuwen Wang [1, #], Jiahao Yu [2, *, #], Yici Liu [3, #]

[1] College of Geography and Environment, Shandong Normal University, Jinan, China

[2] College of Architecture and Urban-Rural Planning, Sichuan Agricultural University, Chengdu, China

[3] School of Geophysics and Geomatics, China University of Geosciences, Wuhan, China

* Corresponding Author Email: 201908211@stu.sicau.edu.cn

[#]These authors contributed equally

Abstract. To address the current situation that urban thermal environment research lacked comprehensive assessment and analysis from natural-social multidimensional factors, this study analyzed the evolution characteristics of thermal environment effects in the central urban area of Chengdu from 2004 to 2019 based on multi-source data. A total of seven influencing factors of natural and social factors that were highly associated with the urban thermal environment were selected, and the influencing factors of spatial differentiation of land surface temperature (LST) and their interactions were studied by applying Geodetector. The results showed that: (1) the heat island in the central city of Chengdu from 2004 to 2019 was radiating outward from the center, and the spatial development spine of the thermal environment remained in the "southeast-northwest" direction, with a significant shift of the center of gravity of the thermal environment from 2011 to 2019; (2) the average LST from 2004 to 2019 increased from 36.57℃to 40.64℃, and the total area of heat island area increased from 641 km^2 to 958 km^2. overall, it showed a shift from sub-medium zone and medium temperature zone to sub-high temperature zone and high temperature zone, and the urban heat island effect tended to enhance; (3) the nighttime light intensity had the largest amount of contribution to the spatial differentiation of LST, and social factors had a more important position relative to natural factors in influencing the urban thermal environment but the amount of contribution from natural factors kept increasing.

Keywords: Thermal environmental effects; Geodetector; spatial heterogeneity; influence factors; Chengdu city.

1. Introduction

The thermal environment is a complex system that can highly summarize and reflect the ecological condition of a city under the joint influence of physical properties of the ground and human socio-economic activities [1]. As urbanization continues to accelerate, the nature of the urban subsurface changes, human activities consume a large amount of fuel, the transmission pathways and efficiency of heat energy within the city change accordingly, and the urban thermal environmental effects are enhanced [2]. The urban thermal environment not only directly affects the health status of urban residents [3], but also has a profound impact on urban energy consumption and ecological sustainability [4]. Therefore, it is important to study the effect of urban thermal environment to optimize the urban ecological environment and increase the sustainable development capacity of cities.

More extensive studies on urban thermal environment effects and their influencing factors have been conducted both domestically and internationally. In terms of natural factors, studies have focused on the effects of changes in landscape patterns such as land use/cover changes, impervious surfaces, and vegetation on the urban thermal environment [5-6]. In terms of social factors, population, economy, and building density and volume ratio have been considered as the main social drivers

affecting the urban thermal environment [7-8]. Although the studies focused on the influence of geographical environmental factors and human activities on the surface thermal environment, there was a lack of quantification of multi-factor effects and the interaction relationships between variables. Geodetector have been widely used in the fields of regional impoverishment [9] and population growth [10] as a novel statistical method to detect spatial differentiation and to reveal the driving forces behind it. It also provides new ideas for quantifying urban thermal environmental impact factors and their magnitude of influence. However, overall, there are few studies that use Geodetector to investigate the combination of multidimensional influencing factors of urban thermal environment, and the cities and regions involved also lack breadth, so the sample size needs to be further expanded. In recent years, Chengdu City has been actively practicing the park city concept while promoting urbanization and promoting the transformation of the city from "outward" to "inward" development, which is somewhat representative.

In summary, this paper explored the thermal environment effect and influencing factors in the central urban area of Chengdu from multiple perspectives based on multi-source data such as LST data, land cover data, nighttime lighting data, and the comprehensive use of standard deviation ellipses and geographic probes. The paper aimed to gain an in-depth understanding of the spatial and temporal evolution of the urban thermal environment, to understand its intrinsic influence mechanism, and to provide a reference basis for mitigating the heat island effect in Chengdu, optimizing the spatial function layout, and promoting the development of park cities.

2. Study area and data

2.1. Study Area Overview

Chengdu, an important city in China, is situated in the central basin plain of Sichuan Province, between 30°05′-31°26′N and 102°54′-104°53′E. The region being examined experiences a climate typified by warm and humid subtropical monsoons that is both warm and humid, with abundant rainfall. On average, the yearly temperature is 16.7℃, with total annual rainfall ranging from 798.3-1541.0mm and an average of 685.5-1002.9h of sunshine per year. Chengdu is composed of 12 districts, 3 counties, and 5 cities at the county level. In 2020, the resident population in Chengdu's central urban area reaches 15,419,400, accounting for 73.64% of the city's resident population. We selected 11 districts as the central urban areas for the study area (Figure.1), including Jinjiang District, Wuhou District and Qingyang District, et al. Its total area is about 3677.70km^2.

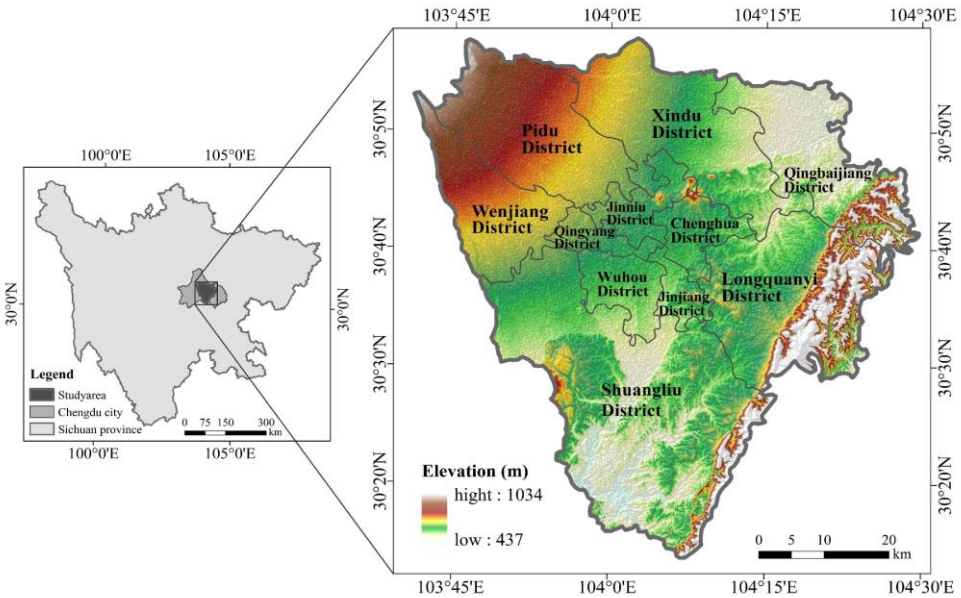


Figure 1. Area of investigation

2.2. Data source and pre-processing

The LST information utilized in this study were obtained from the day-by-day 1 km all-weather LST dataset (TRIMS LST-TP; 2000-2021) V2 [11-14] in western China, and the LST value (°C) was obtained as "image element value/100-273.15" using a raster calculator. Land use data were obtained from the China Land Cover Dataset (CLCD) [15] created by J. Yang et al. of Wuhan University and were classified into nine types: cropland, forest, shrub, grassland, water, snow/ice, barren, impervious surface, and wetland. The nighttime light data were obtained from NOAA's Earth Observation Group (EOG) website, with a unified DN values ranged of 0-63. Information regarding the density of populations were obtained from the WorldPop population density dataset. The data were converted to horizontal Mercator (UTM) projection with an ellipsoid of WGS84. all raster data were unified to 1km except land cover data. land cover data were resampled to 25m to facilitate the statistics of the area share of each category in the 1km×1km grid. Tab.1 displays the data information.

Table. 1 Data situation

Data series	Data name	Time	Data source	Resolution
Raster data	LST data	August 7, 2004; August 8, 2011; August 8, 2019	poles.tpdc.ac.cn	1km
	Land use data	2004; 2011; 2019	https://www.zenodo.org/	30m
	Nighttime lighting data		https://eogdata.mines.edu/products/vnl/	500m/1km
	Population density data		https://hub.worldpop.org/	1km
Vector data	Chengdu City Administrative Boundary Vector Data	2021	http://www.webmap.cn	/

3. Methods

Based on the objectives of this study, this manuscript is organized as presented in Figure 2. The technical flowchart consists of data collection and preprocessing (a), temporal and spatial distribution characteristics in LST (b), spatiotemporal variation in influencing factors (c), and relationship between spatiotemporal variation characteristics of LST and influencing factors (d).

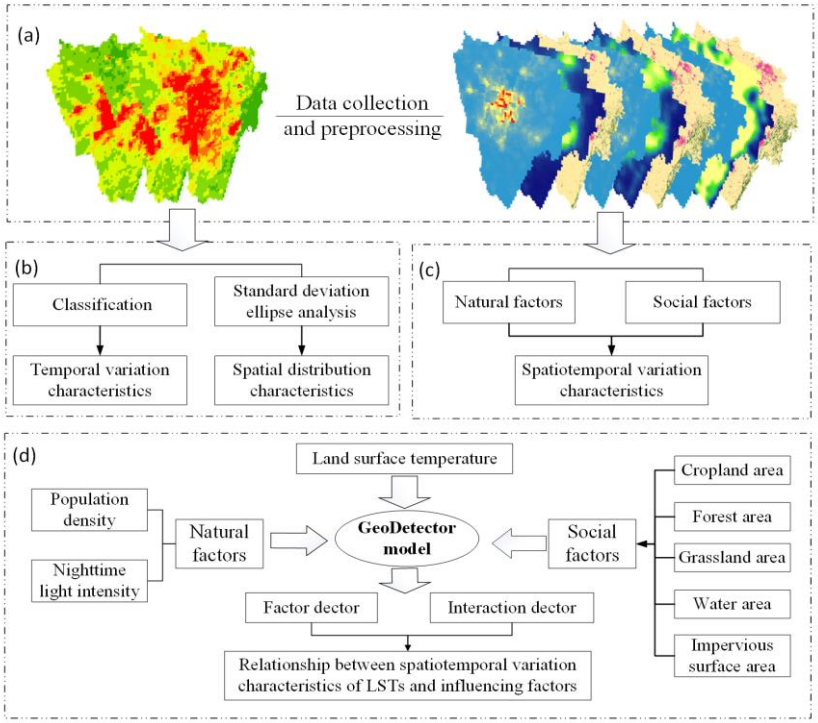


Figure 2. Technical flowchart

3.1. LST classification

The equal spacing and mean-standard deviation methods are commonly used to categorize classes of LST [16]. Within this article, the method of mean-standard deviation is used to differentiate the threshold values by combining them with different multiplicative standard deviations, using the mean value of the temperature of the land surface in the study area. as the base. This method classifies LST into six classes: low, sub-medium, medium, sub-high, high, and extra-high temperature zones. The urban heat island zones are defined as the extra-high and high temperature zones [17]. The criteria for grading are displayed in Table 2. In this table, T_s represents the LST, μ stands for the average LST in the study area, and std denotes the standard deviation.

Table. 2 Classification of LST classes

Heat Island Class	Interval classification criteria
Extra-high Temperature Zone	$T_s > \mu + std$
High Temperature Zone	$\mu + 0.5std < T_s \leq \mu + std$
Sub-high Temperature Zone	$\mu < T_s \leq \mu + 0.5std$
Medium Temperature Zone	$\mu - 0.5std \leq T_s \leq \mu$
Sub-medium Temperature zone	$\mu - std \leq T_s < \mu - 0.5std$
Low Temperature Zone	$T_s < \mu - std$

3.2. Standard deviation ellipse analysis

To better understand the direction of spatial variation in ground LST in Chengdu's central urban area, a standard deviation ellipse is used for analysis. The ellipse of standard deviation is a measure of the direction of change and trend of data distribution and is a statistical approach for summarizing the spatial attributes of geographic elements. such as summarizing the characteristics of central trend, discrete and directional trends. The ellipse of standard deviation is a traditional method for analyzing directional attributes of spatial distributions. The ellipse is constructed by identifying the center of the circle, establishing the rotational angle, and determining the axis length.

3.3. Geodetector

Geodetector is a collection of statistical approaches for identifying spatial variation, as well as revealing the driving forces behind it [18-20], and the Geodetector R language package used in this study is provided by the official Geodetector website (http://www.geodetector.cn/). This study focuses on the application of factor detectors and interaction detectors in Geodetector.

(1) Factor detector

The value metric, expressed as (1), measures the spatial variability of the dependent variable and the impact of probe factors on the spatial variability of LST.

$$q = 1 - \frac{\sum_{h=1}^{L} N_h \sigma_h^2}{N\sigma^2} \tag{1}$$

In equation (1) $h = 1,2,\cdots,L$ is the classification of the variable Y or factor X; N_h and N are the number of cells in the stratum h and the whole area, respectively; σ_h^2 and σ^2 are the variances of the stratum h and the whole area Y values. q has a value range of [0,1], and larger values indicate more pronounced spatial heterogeneity of Y; if the stratification is generated by the independent variable X, larger values of q indicate that the independent variable X has more significant explanatory power for the attribute The stronger the explanatory power of Y, and vice versa, the weaker.

(2) Interaction detector

The Interaction detector determines how much two interactions between distinct factors account for the dependent variable. It evaluates if these factors, when combined, enhance or diminish the dependent variable's explanatory power or if they operate independently based on the standards in

Tab.3.Where $C = q(A \cap B)$; $min(A, B)$ is the minimum of $q(A)$ and $q(B)$; $max(A, B)$ is the maximum of $q(A)$ and $q(B)$.

Table. 3 Factor interaction detection and judgment indicators

Judgment Criteria	Interaction
$C < min\ (A, B)$	Non-linear weakening
$min\ (A, B) < C < max\ (A, B)$	Single-factor nonlinear attenuation
$max\ (A, B) < C$	Two-factor enhancement
$C = A + B$	Independent
$C > A + B$	Non-linear enhancement

The Geodetector possesses the notable benefit of being capable of identifying both numerical and categorical information. In this research, Chengdu city center's LST served as the dependent variable while the influencing factors were the independent variables. They were input into Geodetector to conduct a quantitative analysis of the interpretation power of each impact factor and the interaction characteristics between the impact factors, to study the influencing mechanism of the geographic variation of LST in the center of Chengdu city.

4. Results and Analysis

4.1. Spatial distribution characteristics of urban thermal environmental effects

The spatial distribution of the thermal environment in the central city of Chengdu in 2004, 2011 and 2019 was obtained by reclassifying the LST according to the temperature class classification standard (Figure 3). It can be found that its LST classes showed an irregular circular distribution, and the LST classes changed from the center to the surrounding area. The heat island area was mainly concentrated in the center of the city, where buildings and population were highly concentrated, such as Chunxi Road business district and Wuhou Industrial Park. The low temperature area was mainly concentrated in the Longquan Mountain Range in the southeast. The spatial distribution characteristics of LST levels in the three periods were similar, i.e., the extra-high temperature zone and the high temperature zone covered the built-up areas where buildings and population are concentrated. The low temperature zone and sub-medium temperature zone were mainly distributed in the vegetation-covered areas such as mountain ranges and non-construction land outside the built-up areas, especially in the Longquan Mountain Range, which showed an obvious "cold island" effect. The medium temperature zone and sub-high temperature zone were distributed between the built-up areas and the peripheral non-built-up land. Comparing the three time series maps, we can see that the extension of the urban heat island area was roughly in the same direction as the expansion of the urban built-up area.

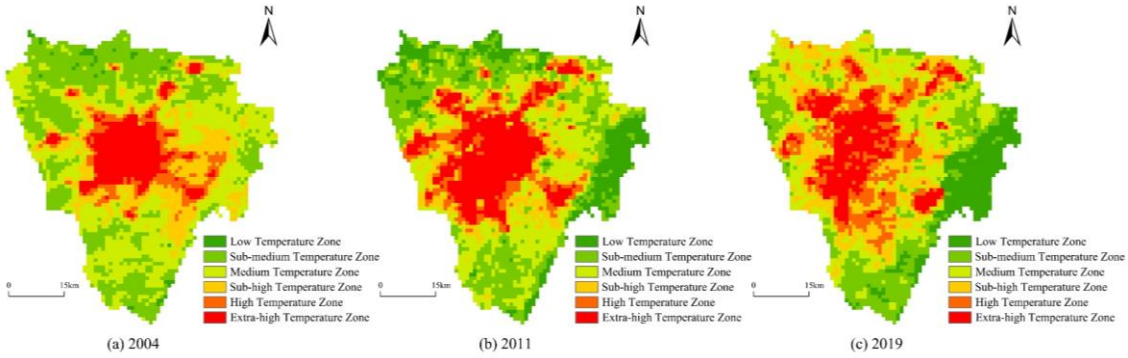


Figure 3. Spatial distribution of LST classes in the central city of Chengdu

The change in the direction of the thermal environment and the migration of the center of gravity in the central city of Chengdu were plotted (Figure 4). From the figure, it can be seen that the spatial

development axis of thermal environment in the study area from 2004 to 2019 was maintained in the "southeast-northwest" direction. From the distribution and migration trajectory of the center of gravity, the center of gravity of LST from 2004 to 2019 was located in Jinjiang District, and the center of gravity of the thermal environment migrated to the northwest with a distance of 911.219 meters. Among them, the center of gravity of the thermal environment shifted 336.08 m to the northwest from 2004 to 2011, with a deflection angle of 6.7°. The migration was more obvious from 2011 to 2019, with the center of gravity of the thermal environment shifting 575.14 m to the northwest, with a deflection angle of 46.3°. The reason for this feature may be that the development of the core circle of Chengdu City has slowed down and some industries have migrated to the second circle.

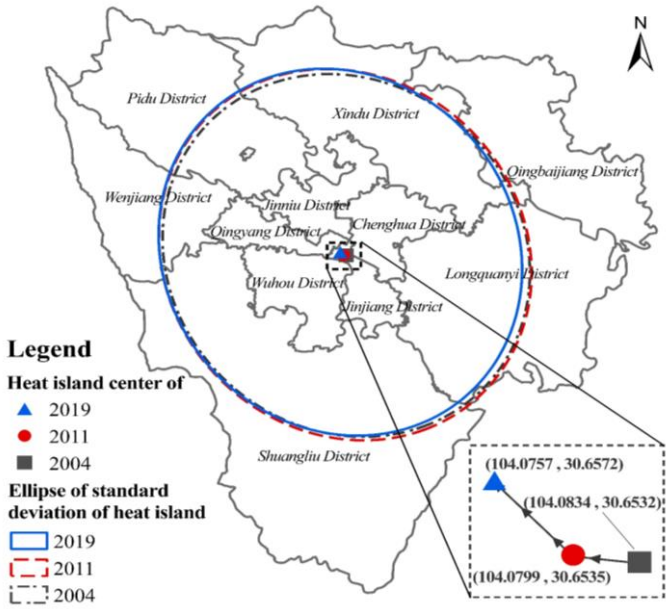


Figure 4. Standard deviation ellipse of LST in the central city of Chengdu

4.2. Temporal evolution characteristics of urban thermal environmental effects

The average LST in the central city of Chengdu in 2004, 2011 and 2019 was 36.57℃, 36.98℃ and 40.64℃, with a small increase from 2004 to 2011 and a significant change in the average LST from 2011 to 2019 with an increase of 3.66℃. The area and proportion of each temperature class sub-area were counted in 2004, 2011 and 2019 (Figure 5). The percentage of the low temperature zone was 1.16%, 12.55% and 11.22% in 2004, 2011 and 2019, respectively. The proportion of sub-moderate temperature zone area decreased by 12.86%, and the main trend from 2004 to 2011 was the transformation of sub-medium temperature zone to medium temperature zone. The area of the medium temperature zone was 1204 km^2 in 2004, reduced to 847 km^2 in 2011 and 822 km^2 in 2019, with the largest area proportion in all three periods. The sub-high temperature zone showed a fluctuating change of decreasing and then increasing from 2011 to 2019, with an overall increasing trend, with an increased area of 162km^2, accounting for 4.69% increase. The total area of the heat island zone was 641 km^2 in 2004, and increased to 948 km^2 in 2011, with an increase of 47.9%, and increased less from 2011 to 2019, with 958 km^2 in 2019. From 2004 to 2019, the percentage of the heat island zone increased from 18.53% to 27.69%. Among them, the area of the high temperature zone showed a continuous increase, with an increase of 227km^2 or 88.3% from 2004-2019. The area of the extra-high temperature zone was 384km^2 in 2004, increased to 631km^2 in 2011, and decreased to 474km^2 in 2019, showing a fluctuating change of increase and then decrease, but the overall trend of growth. Overall, the area of the sub-moderate and moderate temperature zone shifted to the sub-high and high temperature zones from 2004-2019. Therefore, although the change in the area of heat island zone was not obvious in 2011-2019, there was still a tendency for the heat environment effect to increase.

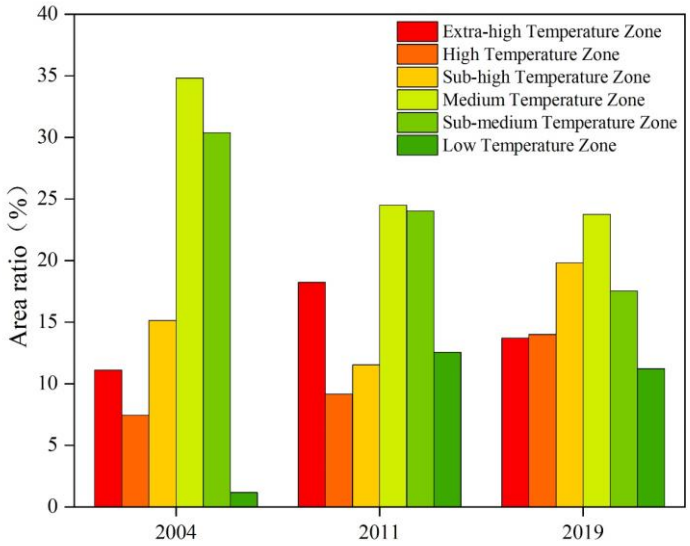


Figure 5. Percentage of LST classes in the central city of Chengdu

4.3. Temporal evolution characteristics of urban thermal environmental effects

This paper selected relevant natural factors (cropland area, forest area, grassland area, water area, impervious surface area, etc.) and social factors (population density, nighttime light intensity) as thermal environment influencing factors according to the characteristics of urban construction in Chengdu and analyzed their spatial distribution characteristics and temporal change trend. The spatial distribution of the thermal environment influencing factors in the central city of Chengdu at different periods is shown in Figure 6.

As shown in Figure 6 (a) (b) (c), the land use types in the study area were mainly cropland, impervious surface, and forest. From 2004 to 2019, the area of cropland was decreasing year by year. Compared with 2570.27 km^2 in 2004, the area of cropland decreased by about 490.42 km^2 in 2019, and the proportion decreased from 86.24% to 69.79%. The forest area reached 101.91 km^2 in 2019, nearly doubling from 51.63 km^2 in 2004. The increase in impervious surface area was more significant, from 339.00 km^2 in 2004 to 773.69 km^2 in 2019, with the percentage increasing from 11.37% to 25.96%. The area changes of grassland, water and barren were relatively stable. According to the trend of land use change it can be shown that from 2004 to 2019, in the urbanization and construction of Chengdu city, the expansion of construction land was obvious and the cropland was seriously damaged. From Figure 6 (d) (e) (f), the population density in the central area of Chengdu increased year by year, and there was a population clustering effect in all urban centers. Compared with 2004 and 2011, the population clustering effect was more significant in 2019. As shown in Figure 6(g) (h) (i), the nighttime light intensity was related to the expansion of the construction area. The range of high values of nighttime lights (DN value = 63) had been expanding, mainly concentrated in the core area of the city in 2004 and covering almost the whole study area in 2019. This indicated that the scope and intensity of socioeconomic activities in Chengdu were expanding, which was basically consistent with the changes in LST.

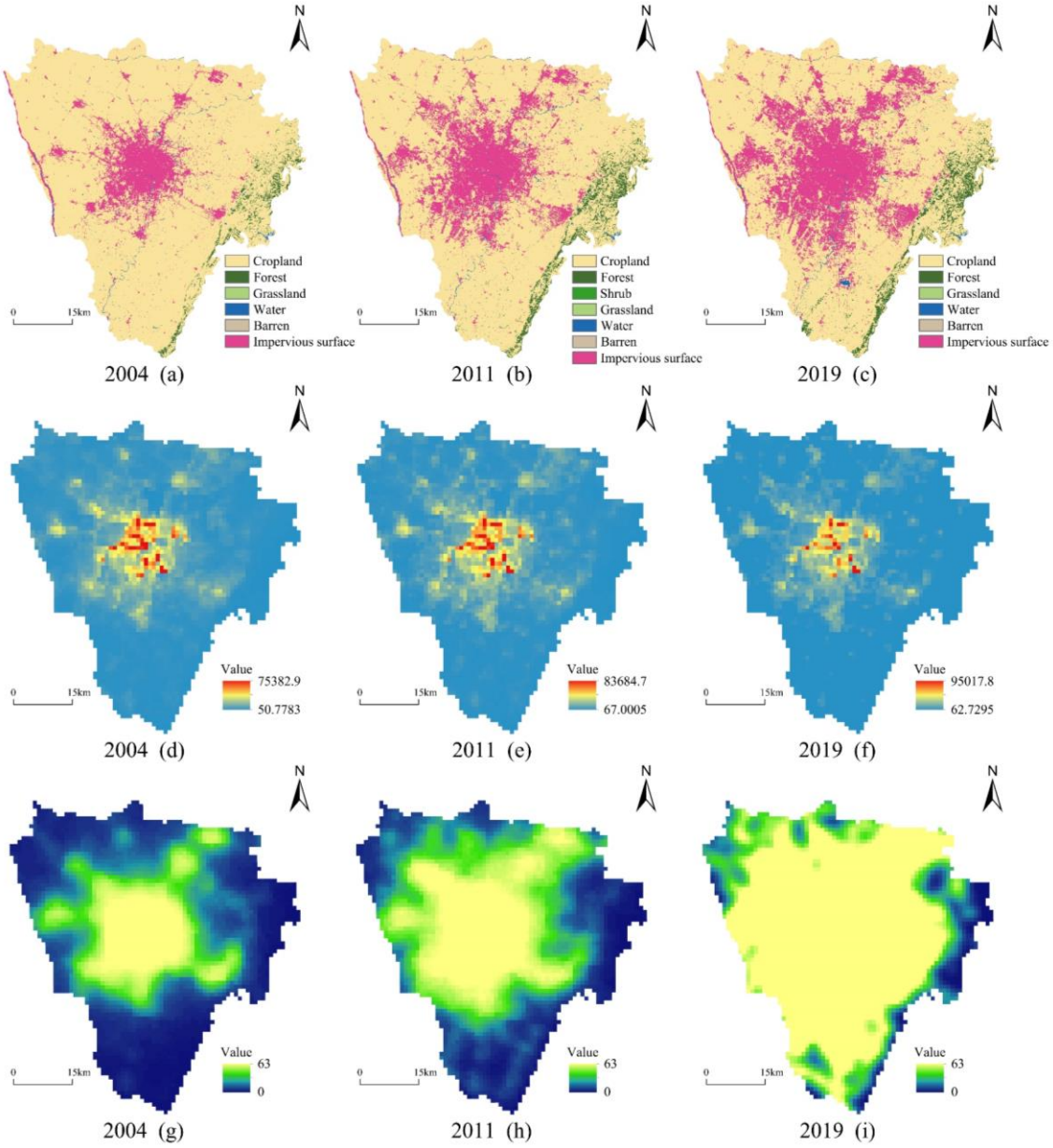


Figure 6. Spatial distribution of thermal environment influencing factors

4.4. Geodetector detection results

The factor detector and interaction detector functions of the Geodetector were used to analyze the degree of explanation that each influence factor effected on the spatial divergence pattern of LST in the central city of Chengdu from 2004 to 2019. Among them, X1, X2, X3, X4, X5, X6 and X7 represented population density, nighttime light intensity, cropland area, forest area, grassland area, water area and impervious surface area, respectively.

4.4.1 Single factor effect analysis

The relative importance among the influencing factors, i.e., the contribution of each influencing factor to the LST change in the central urban area of Chengdu, q, was detected using a factor detector, and the obtained results are shown in Figure 7. The contribution of each influence factor to the change of LST was ranked sequentially as shown below:

(1)2004: X2 (63.8%) > X7 (62.5%) > X3 (58.2%) > X1 (48.6%) > X5 (2.3%) > X4 (1.6%) > X6 (0.9%);

(2)2011: X2 (69.7%) > X7 (66.8%) > X1 (52.3%) > X3 (49.3%) > X4 (16.6%) > X5 (9.9%) > X6 (0.5%);

(3)2019: X2 (88.7%) > X7 (51.4%) > X1 (40.0%) > X4 (32.2%) > X3 (30.7%) > X5 (8.4%) > X6 (0.5%)

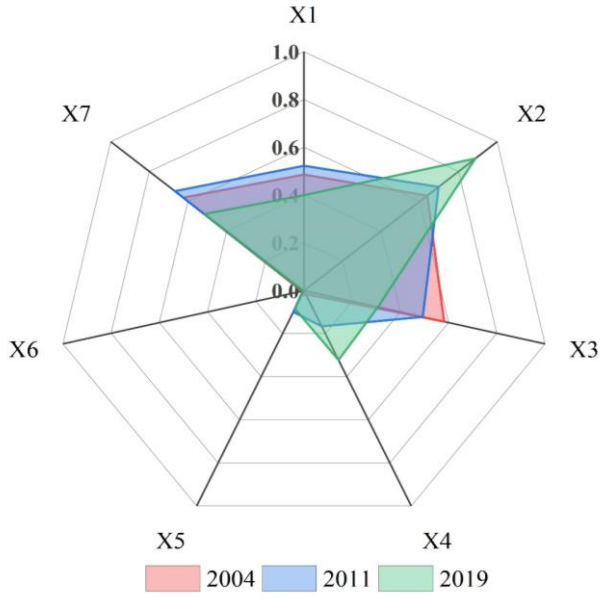


Figure 7. Factor detector results

The effect of each factor on the change of LST was analyzed in conjunction with Figure 7. The contribution of nighttime light intensity always ranked first, and the q-values were all greater than 60%, indicating that human living and production activities played an important role in the changes of LST; The contribution of water area to LST change in the central urban area of Chengdu was the smallest, with q value less than 1%. Considering the small total area of water in the main urban area, the effect of water on LST change was regarded as not signification. The contribution difference between grassland area and population density was large, which detected natural factors and social factors that contributed the least to the change of LST in the main urban area. It indicated that natural factors and social factors differ greatly in the intensity and mode of influence on LST change in Chengdu city center, and social factors played a leading role in the influence of LST change in Chengdu city center. The largest contribution of natural factors, impervious surface area, was greater than the q value of population density, indicating that not all social factors have had a dominant effect on LST change in the central urban area of Chengdu in recent years, and the impact of natural factors on the effect of urban thermal environment cannot be ignored as well. From 2004 to 2019, the distribution pattern of the q-value of the contribution of each influence factor in the radar plot had changed obviously, which indicated that the factors that affected the urban thermal environment were also changing dynamically, and the balance between the influence of natural factors and human activity factors became more and more important, with the development of the urbanization.

4.4.2 Interaction analysis of different influencing factors

The interaction of influencing factors of LST change in central urban area of Chengdu was analyzed using the interaction detector. The results of the interaction with the detector are shown in Figure 8. Among them, the diagonal values are the degree of explanation of each driving force, and the non-diagonal line is the degree of explanation after the interaction of two influence factors.

2004	X1	X2	X3	X4	X5	X6	X7
X1	0.490	0.654	0.674	0.492	0.491	0.515	0.664
X2	0.654	0.638	0.711	0.644	0.643	0.650	0.708
X3	0.674	0.711	0.587	0.621	0.589	0.605	0.641
X4	0.492	0.644	0.621	0.016	0.040	0.026	0.628
X5	0.491	0.643	0.589	0.040	0.023	0.021	0.631
X6	0.515	0.650	0.605	0.026	0.021	0.009	0.643
X7	0.664	0.708	0.641	0.628	0.631	0.643	0.625

2011	X1	X2	X3	X4	X5	X6	X7
X1	0.523	0.719	0.664	0.553	0.594	0.539	0.696
X2	0.719	0.697	0.761	0.710	0.739	0.705	0.756
X3	0.664	0.761	0.493	0.690	0.548	0.508	0.697
X4	0.553	0.710	0.690	0.166	0.234	0.168	0.695
X5	0.594	0.739	0.548	0.234	0.099	0.105	0.694
X6	0.539	0.705	0.508	0.168	0.105	0.005	0.677
X7	0.696	0.756	0.697	0.695	0.694	0.677	0.668

2019	X1	X2	X3	X4	X5	X6	X7
X1	0.400	0.470	0.527	0.509	0.475	0.432	0.558
X2	0.470	0.887	0.552	0.437	0.359	0.335	0.556
X3	0.527	0.552	0.307	0.604	0.376	0.337	0.592
X4	0.509	0.437	0.604	0.322	0.368	0.324	0.609
X5	0.475	0.359	0.376	0.368	0.084	0.093	0.546
X6	0.432	0.335	0.337	0.324	0.093	0.005	0.534
X7	0.558	0.556	0.592	0.609	0.546	0.534	0.514

	Enhance,non-linear
	Enhance,bi-factor
	Weaken,monofactor,linear
	Factor detector

Figure 8. Factor interaction results

Combined with Figure 8, the result of the interaction of influencing factors on the LST change in the central urban area of Chengdu has been analyzed. There were three types of interactions on LST in the central urban area of Chengdu, including two-factor enhancement, non-linear enhancement, and single-factor non-linear attenuation. The two-factor enhancement had the most interactions, indicating that in most cases, any two factors superimposed on each other will have a stronger driving effect on the thermal environmental effects. In 2004, the driving force interaction on the thermal environmental effect in the central urban area of Chengdu showed a two-factor enhancement overwhelmingly, and the interaction between grassland area and water area showed a one-factor non-linear weakening effect, indicating that the interaction between grassland and water had a certain mitigation effect on the further enhancement of the thermal environmental effect. In 2011, the two-factor enhanced interaction effect of nighttime light intensity and cropland area had the highest influence of 0.761. Meanwhile nighttime light intensity ∩ population density, population density ∩ impervious surface area, population density ∩ water area, impervious surface area ∩ cropland area, cropland area ∩ forest area showed non-linear enhancement after interaction, and the driving effect on the thermal environment effect in the central city of Chengdu grew significantly. In 2019, nighttime light intensity showed a one-way nonlinear attenuating effect when interacting with other factors, indicating that nighttime light intensity in that year attenuates the effect of nighttime lights on the thermal environment effect in the central city of Chengdu when interacting with other factors. Therefore, the effect of thermal environmental was not only a certain factor solely influenced, but also influenced by the joint action of many factors. The combination and quantity of each influencing factor could be optimized to achieve the purpose of mitigating and improving the thermal environmental effect.

5. Conclusion

This study addressed the characteristics of urban thermal environmental effects research such as data sources and analysis of influencing factors were relatively single and took the rapidly urbanizing

Chengdu city as an example to obtain the spatial heterogeneity of LST and its influencing factors in the central urban area of Chengdu city from 2004 to 2019 based on multi-source data. On this basis, the spatial heterogeneity and influence mechanism of the thermal environmental effect in the central urban area of Chengdu city were applied to the geographic probe and provided a reference basis for mitigating the thermal environmental effect in Chengdu city and promoting urban ecological protection and sustainable development. The conclusions of the study were as follows:

(1) In terms of spatial scale, the heat island area in the central urban area of Chengdu was mainly concentrated in the urban center where buildings and population were highly concentrated. Urban heat island radiates was outward, and its expansion direction was basically consistent with urban built-up area from 2004 to 2019, the main axis of the thermal environment was maintained in the "southeast northwest" direction, with the center of gravity of the thermal environment shifting more obviously from 2011 to 2019.

(2) In terms of time scale, the average of LST in the central urban area of Chengdu was 36.57°C, 36.98°C and 40.64°C in 2004, 2011 and 2019 respectively. From 2011 to 2019, with the average LST went up, they increased by 3.66°C. The total area of the heat island zone in the central urban area of Chengdu increased from 641 km^2 in 2004 to 958 km^2 in 2019, but the increase was smaller from 2011 to 2019. Overall, it had been changed from sub-medium temperature zone and medium temperature zone to sub-high temperature zone and high temperature zone, and although the increase in heat island area from 2011-2019 was not significant, the urban heat island effect tended to enhance.

(3) The Geodetector results showed that, from the perspective of the contribution of each influencing factor, nighttime light intensity was the factor that contributed most to the LST change in the central urban area of Chengdu, and social factors had a more important position than natural factors in influencing the thermal environment effect in the central urban area of Chengdu, but the influence of natural factors on the LST of the city should be appreciated as well. From the perspective of the interaction, the factors had an interactive effect and worked together to cause changes in LST, and in most cases any two factors superimposed on each other will have a more powerful contribution to the thermal environmental effect in Chengdu.

Due to the lack of data and inapplicability in the study area, only a portion of the influencing factors affecting temperature change were counted in this study. We quantitatively analyzed the relative importance of natural and social factors in influencing LST changes and their effects on LST changes. Then, we analyzed the effects of human activities and changes in the natural environment. In recent years, the degree of influence of anthropogenic factors on the natural environment has been increasing, and the interaction and influence between social factors and natural factors, and the criteria for dividing social factors and natural factors are no longer absolute. In this study, the influencing factors of urban LST change were analyzed in terms of their contributions, while the inner mechanism of urban thermal environment needed to be further studied in order to construct an urban thermal environment response model with universal applicability.

References

[1] Yu W, Xu J, Xu L. An analysis on eco-environmental effect of urban land use based on remote sensing images: a case study of urban thermal environment and NDVI [J]. Acta Ecologica Sinica, 2006, 26(5): 1450-1460.

[2] Shen Q, Zhang X, Zhou Y. Urban Ecological Crisis: Characteristics, Factors and Analysis [J]. Urban Planning Forum, 2012(6): 23–33.

[3] Kovats RS, Hajat S. Heat Stress and Public Health: A Critical Review [J]. Annu Rev Public Health, 2008, 29: 41–55.

[4] Grimm NB, Faeth SH, Golubiewski NE, Redman CL, Wu J, Bai X, et al. Global Change and the Ecology of Cities [J]. Science, 2008, 319(5864): 756–760.

[5] Bokaie M. Assessment of Urban Heat Island Based on the Relationship between and Land Use/Land Cover in Tehran [J]. Sustainable Cities and Society. 2016, 23: 94–104.

[6] Wang Y, Wu J, Li W, Li Z. Study on land surface temperature vegetation cover relationship in urban region: a case in Shenzhen City [J]. Geographical Research, 2006, 25(3): 369-377+561.

[7] Li Y, Sun Y, Li J, Gao C. Socioeconomic drivers of urban heat island effect: Empirical evidence from major Chinese cities [J]. Sustainable Cities and Society, 2020, 63.

[8] Mitchell BC, Chakraborty J. Urban Heat and Climate Justice: A Landscape of Thermal Inequity in Pinellas County, Florida [J]. Geographical Review, 2014, 104(4): 459–480.

[9] Zhou P, Deng W, Zhang S, Meng B. Evolution Characteristics and Its Driving Force of Territory Space Pattern in the Taihang Mountain, China [J]. Mountain Research, 2020, 38(2): 276–289.

[10] Luo J, Shi P, Zhang X. Population distribution and influencing factors in Lanzhou-Xi'ning urban agglomeration based on township scale [J]. Journal of Arid Land Resources and Environment, 2020, 34(7): 104–111.

[11] Zhou J, Zhang X, Tang W, Ding L, Ma J, Zhang X. Daily 1-km all-weather land surface temperature dataset for Western China (TRIMS LST-TP; 2000-2021) V2. 2019.

[12] Zhang X, Zhou J, Liang S, Wang D. A practical reanalysis data and thermal infrared remote sensing data merging (RTM) method for reconstruction of a 1-km all-weather land surface temperature [J]. Remote Sensing of Environment. 2021, 260.

[13] Zhang X, Zhan W, Liu S, Cao R. A Method Based on Temporal Component Decomposition for Estimating 1-km All-Weather Land Surface Temperature by Merging Satellite Thermal Infrared and Passive Microwave Observations [J]. IEEE TRANSACTIONS ON GEOSCIENCE AND REMOTE SENSING, 2019, 57(7): 4670-4691.

[14] Zhou J, Zhang X, Liu S, Olesen FS, Hu W, Dai F. A Thermal Sampling Depth Correction Method for Land Surface Temperature Estimation from Satellite Passive Microwave Observation Over Barren Land [J]. IEEE TRANSACTIONS ON GEOSCIENCE AND REMOTE SENSING, 2017, 55(8): 4743–4756.

[15] Yang J, Huang X. The 30 m annual land cover dataset and its dynamics in China from1990 to 2019 [J]. Earth System Science Data, 2021, 13(8): 3907-3925.

[16] Chen S, Wang T. Comparison Analyses of Equal Interval Method and Mean-standard Deviation Method Used to Delimitate Urban Heat Island [J]. Journal of Geo-information Science. 2009, 11(2): 145–150.

[17] Yao X, Wang X, Yao X. Thermal environmental effect of the main urban area of Fuyang City in northern Anhui based on RS technology [J]. Chinese Journal of Ecology, 2021, 40(10): 3290–3303.

[18] Wang J, Li X, Christakos G, Liao Y, Zhang T, Gu X, et al. Geographical Detectors-Based Health Risk Assessment and its Application in the Neural Tube Defects Study of the Heshun Region, China [J]. International Journal of Geographical Information Science, 2010, 24(1): 107-127.

[19] Wang J, Zhang T, Fu B. A measure of spatial stratified heterogeneity [J]. Ecological Indicators, 2016, 67: 250–256.

[20] Wang J, Xu C. Geodetector: Principle and prospective [J]. Acta Geographica Sinica, 2017, 72(01): 116–134.